Computer Simulation Study of Bulk Atactic Polystyrene in the Vicinity of the Glass Transition

*Alexey V. Lyulin, J.J. de Groot, M.A.J. Michels**

Group Polymer Physics, Department of Applied Physics and Dutch Polymer Institute, Technische Universiteit Eindhoven, P.O. Box 513 5600 MB Eindhoven, The Netherlands

Summary: Molecular dynamics (MD) simulations of bulk atactic polystyrene have been performed in a temperature range from 100 K to 650 K at atmospheric pressure. Local translational mobility has been investigated by measuring the mean square translational displacements of monomers. The long-time asymptotic slope of these dependencies is 0.54 at $T>T_g$, showing Rouse behavior. Cross-over from motion in the cage to Rouse like dynamics has been studied at $T>T_g$ with a characteristic cross-over time follows a power law behavior as a function of T, as predicted by mode-coupling theory (MCT). Local orientational mobility has been studied via the orientational autocorrelation functions, ACFs, (Legendre polynomials of the first and second order) of both the main-chain and side-group bonds. The relaxation times of the orientational α-relaxation follow the same power law (γ~2.9) as the characteristic translational diffusion time. Below T_g both types of dynamics are described by the same activated law. The ACFs time-distribution functions reveal the existence of activated local rearrangements already above T_g.

Keywords: amorphous; glass transition; molecular dynamics;; polystyrene; relaxation

Introduction

Dynamical characteristics of amorphous polymers in the glassy state control such important properties as ductility, toughness and impact resistance. It has recently become clear that the yield behavior of amorphous polymers (polystyrene, PS, as an important example) is intimately linked to collective segmental dynamics of individual or neighboring chains[1]. Relaxational processes in amorphous PS in the vicinity of T_g have been studied experimentally by dynamic mechanical[1-3], quasielastic neutron scattering[4,5], dielectric[6-12] and NMR techniques[13-16]. It is an established fact that above the PS glass-transition temperature (T_g = 373 K), the α-relaxation is the primary relaxation process of collective segmental motion[17], and the temperature dependence of the characteristic relaxation times is well described by WLF equation[18]. Apart from the investigation of the rotational mobility, local translational mobility has been studied in the very detailed

 CCC 1022-1360/00/$ 17,50+.50/0

quasielastic neutron scattering experiments of Kanaya et al.[5], in the very broad temperature range of 21-475 K covering the glass transition temperature. In the time dependence of the mean-square proton translational displacements two distinct regimes were found: the short time regime for times $t<5$ ps associated with a segment motion in the cage formed by the neighboring segments, and some slower regime as expected for the Rouse behavior. These findings have been recently confirmed by computer simulation studies of Roe et al.[19,20], and by more extensive MD simulations of Lyulin and Michels[21,22].

Increasing of the relaxation times by many orders of magnitude when approaching glass transition is reasonably well described in general by the mode-coupling theory (MCT) of supercooled liquids[17,23-27]. The ideal form of MCT predicts a dynamical critical temperature T_c at which the molecules become permanently trapped in some cage formed by their almost frozen neighbors.

The general aim of our studies is to understand the differences in local segmental dynamics in different amorphous polymer melts above and below the glass transition by computer simulation, and to make the connection with chemical structure. In this paper we focus on the analysis of both local translational and rotational mobility for a realistic model amorphous polymer melt and on comparison with the predictions of MCT. For some low temperatures we thereby performed more simulations and managed to increase the simulated times up to 0.1 μs.

Simulation details

The united-atom model of PS of our previous study[21,22] is explored also in the present paper. The model consists of a single polymer chain of $N_p = 80$ monomers (molecular weight ~ 9000) and its periodic images generated by periodic boundary conditions. The stereochemic configurations of the aromatic groups were generated at random so that the ratio of number of *meso* to number of *racemic* dyads was near unity. All potential contributions and potential constants in the force field are identical to [21]. The length of all valence bonds has been constrained by the SHAKE iterative procedure[28], with a relative tolerance of 10^{-6}.

The leap-frog variant of the velocity Verlet algorithm[29] has been used to integrate the Newtonian equations of motion. For the present calculations well-equilibrated initial structures have been taken from the previous study[21]. Some runs have been performed using initial structures generated by the MSI Materials Studio™ Amorphous Cell interface. Berendsen thermostat and barostat[29] were used to keep the system at prescribed temperatures and pressures. The production

runs have been performed by NVE MD with the integration step of $\Delta t = 2 - 2.5$ fs.

Local Translational Mobility

Local translational mobility has been studied by measuring the mean-square translational displacements of individual beads in the main chain and in the side phenyl groups. At very small times (t<1-3 ps) the regime of free monomer diffusion, with a slope of about 1, takes place. In a high-temperature melt, when $T >> T_g$, this regime changes into a second diffusive regime, with the slope about 0.5, which confirms a well-known prediction for the Rouse chain. With decreasing the temperature the motion of the chain bead is becoming more and more restricted: the onset of the second diffusion is preceded by some plateau. This plateau is connected with the cage effect, whereby very restricted local motions occur in the cage formed by surrounding monomers.

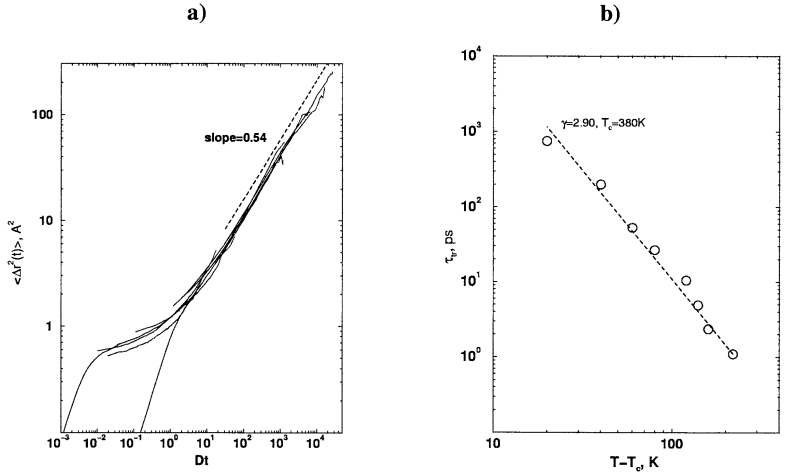

Figure 1. a) Mean-square displacement as a function of Dt for different temperatures. An asymptotic slope of 0.54 is shown by the dashed line.
b) Temperature dependence of the translational relaxation times $\tau_{tr}=D^{-1}$. Straight line is fit according to Eq. 2 using T_c = 380 K.

As suggested by van Zon and de Leeuw in their study of a model polymer melt without chemical details[23], the idealized MCT for the translational α-relaxation may apply, which predicts that the final parts of the mean-square translational displacements curves can be fitted with the power law

$$\left\langle \Delta r^2(t) \right\rangle \sim (Dt)^{\alpha}, \tag{1}$$

where D is a diffusion constant in the regime of the Rouse diffusion. Averaging the exponents α for different temperatures gives $\alpha = 0.54 \pm 0.04$. The mean-square displacements are plotted as functions of Dt at different temperatures in Figure 1a, showing this scaling behavior.

According to the MCT the characteristic time of the α-relaxation, $\tau_{tr} = D^{-1}$ algebraically diverges at some critical temperature T_c just above T_g:

$$\tau_{tr} = \frac{\tau_0}{(T - T_c)^{\gamma}}. \tag{2}$$

Different exponents γ have been obtained in some previous simulations[23-25]. Using the simple bead-spring model Bennemann et al.[24,25] found $\gamma = 2.1 - 2.3$. For a model polymer with angle and torsion potentials van Zon and de Leeuw[23] obtained $\gamma = 2.85$. Fitting with the straight line in

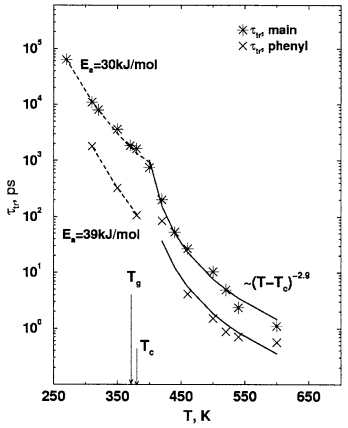

Figure 2. Temperature dependence of the translational relaxation times $\tau_{tr}=D^{-1}$ both for the beads in the main chain and in the side group. Solid line is the MCT-based fit, Eq. 2. Dashed line is the fit with the simple activation law, Eq. 3.

Figure 1b we find that the power law (2) holds for few orders of magnitude and gives $T_c = 380$ K and $\gamma = 2.90$. This value of T_c is somewhat higher than the observed glass transition temperature $T_g \sim 370$K, as predicted by MCT. The value of γ is in a very good agreement with the value of $\gamma =$

2.85 obtained by van Zon and de Leeuw[23] for the model polymer melt. The larger value of γ as compared to the results of Benneman et al.[24,25] shows the influence of intramolecular interactions on the slowing down of dynamics in the vicinity of the glass transition.

The temperature dependence of $\tau_{tr} = D^{-1}$ is for the full temperature range shown in Figure 2; as already mentioned at $T>T_g$ this dependence is well described by MCT (solid lines in Figure 2). At $T<T_g$ clearly different behavior is observed for the onset of the second diffusion regime; a simple activation law is used to fit the data for both the main-chain and side-group translational-diffusion times (dashed lines in Figure 2),

$$\tau_{tr} \sim \exp(E_a / k_B T). \tag{3}$$

This gives for the activation energy the values $E_a \sim 30$ kJ/mol (main chain) and $E_a \sim 39$ kJ/mol (phenyl group).

Local Orientational Mobility

To have insight into possible common mechanisms of the different types of segmental mobility (translational and rotational) and in order to compare the results with the predictions of MCT, the local orientational mobility has been studied with the help of Legendre polynomials of the first and second order (autocorrelation functions, ACFs)

$$\begin{aligned} P_1(t) &= <\mathbf{b}(0)\mathbf{b}(t)> \\ P_2(t) &= <3/2(\mathbf{b}(0)\mathbf{b}(t))^2 - 1/2> \end{aligned}, \tag{4}$$

where **b** is the unit vector directed along the main-chain bond or along the phenyl side group and brackets denote the time averaging. A decrease of temperature leads to a pronounced slowing down of the orientational mobility both for the P_1 and P_2 ACFs. The orientational relaxation for the bond in the middle of the chain is almost frozen in the vicinity of T_g. The phenyl side groups are more mobile as compared to the bonds in the main chain at the same value of temperature.

KWW stretched exponents have been used to fit the P_1 and P_2 ACFs at different values of temperature,

$$P_{1,2}(t) = \exp(-(t/\tau_{1,2})^{\beta}), \tag{5}$$

where $\tau_{1,2}$ is the characteristic relaxation time and β is the parameter effectively taking into account the non-exponential nature of the relaxation process. At low temperatures, $T < T_g$, the relaxation of P_1 and P_2 ACFs is far from complete, but nevertheless the fits are good and allow to

determine relaxation times which are much larger than the actual length of the simulation run. The temperature dependence of the relaxation times $\tau_{1,2}$ is shown in Figure 3. In the melt, when $T>T_g$, the T-dependence is clearly non-Arrhenius; its shape is similar to the experimentally observed α-process.

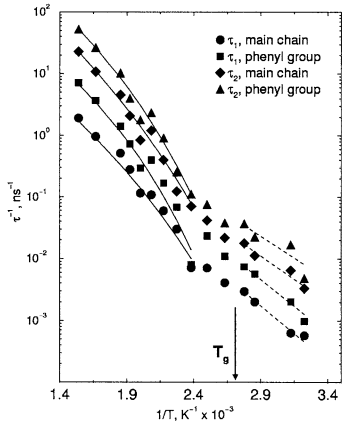

Figure 3. Temperature dependence of the relaxation times $\tau_{1,2}$ of the $P_{1,2}$ ACFs. Solid lines are Vogel-Fulcher fits, Eq. 6, to the data at $T>T_g$. Dashed lines are fits with the simple activation law at $T<T_g$.

From the Vogel-Fulcher fit,

$$\tau_{1,2}^{-1} \sim \exp(-E_a / k_B(T - T_0)), \tag{6}$$

quite similar results have been obtained, $E_a \sim 10$ kJ/mol and $T_0 \sim 300$ K (essentially lower than T_g), for the P_1 and P_2 ACFs, both for the main chain and side groups. At low temperature, $T < T_g$, the T-dependence of the relaxation times shows different behavior and is described as a simple activation process with an activation energy (averaged for all four data sets in Figure 3) $E_a = 31$ kJ/mol. This value of the activation energy is close to the value $E_a \sim 30$ kJ/mol observed earlier for the onset of the second translational diffusion regime at $T<T_g$, associated with the escape from the particle's cage.

We also have tried to fit the temperature dependence of the relaxation times $\tau_{1,2}$ at $T>T_g$ with the power-law fits of (2) predicted by MCT for the α-relaxation, Figure 4a. The fits give the same

value of the critical temperature, T_c=*380K*, as in the case of the translational diffusion. The

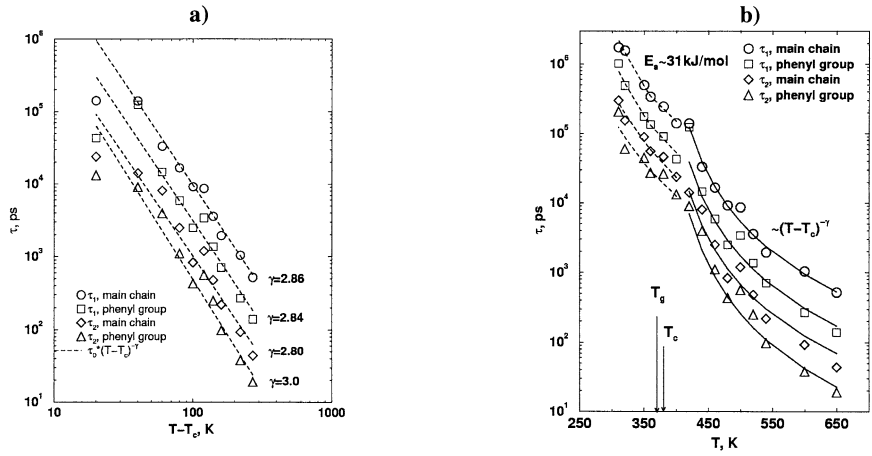

Figure 4. a) Temperature dependence of the relaxation times $\tau_{1,2}$ of the $P_{1,2}$ ACFs at $T>T_g$. Straight lines are fits according to Eq. 2 using T_c=*380 K*.
b) Temperature dependence of the relaxation times $\tau_{1,2}$ of the $P_{1,2}$ ACFs both for the main chain and the side group. Solid lines are the MCT-based fits, Eq. 2. Dashed lines are the fits with the simple activation law.

average exponent $\gamma = 2.88$ is very close to the values of 2.90 for τ_{tr}.

To complete the picture we plot $P_{1,2}$ orientational relaxation times as functions of temperature, Figure 4b, as we did earlier for translational relaxation times $\tau_{tr} = D^{-1}$ in Figure 2. Qualitatively the picture of reorientational relaxation is very similar to the translational relaxation: the *T*-dependence of the characteristic relaxation times is changed from the algebraic dependence described by MCT, Eq. 2, to the simple activated process, Eq. 3, both for the translational and orientational relaxation. The values of the critical temperature T_c, power γ and activation energy E_a are very close for both types of mobility, orientational and translational. We can generally conclude here that the predictions of MCT hold at $T>T_g$ for both types of mobility.

Distribution of relaxation times

Each orientational ACF can be analyzed using the CONTIN[30,31] method and can be represented as

$$ACF(t) = \int_{-\infty}^{+\infty} F(\ln\tau)\exp(-t/\tau)d\ln\tau\,, \qquad (7)$$

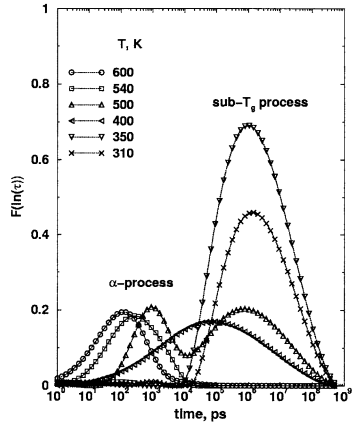

Figure 5. Temperature dependence of the normalized distribution function of the relaxation times for the P_2 ACF for the average bond in the middle of the backbone. Two peaks correspond to two different relaxation processes, diffusive and local activated rearrangement.

where $F(\ln\tau)$ is a normalized distribution function of relaxation times. The distribution function of relaxation times for the P_2 ACF is shown in Figure 5 for the main-chain bond. The distribution functions for the main-chain bond and side phenyl group qualitatively are very similar: at high temperature these functions are unimodal, with the location of the peak shifted towards larger times with decreasing temperature. At T = 500 K the form of the distribution function is becoming bimodal, with one peak located at $\tau \sim 1$ ns and another corresponding to a very slow process at $\tau \sim 10^3$ ns. At T = 400 K analysis reveals a very broad distribution of relaxation times, which could be due to the merging of α- (main structural) relaxation and sub-T_g relaxation processes at this temperature. At lower temperatures, $T<T_g$, the distribution function again becomes unimodal, with a single peak at extremely large values of relaxation times, $\tau > 10^3$ ns.

Conclusion

Using the model from our previous study[21] we have investigated the local dynamical properties of an atactic-polystyrene melt in the vicinity of the glass transition, $T_g \sim 370$ K. Translational mobility has been investigated by using the mean-square displacements of different beads. The

slowing down near T_g of the translational mobility is mainly explained by the existence and diffusion of cages formed by their almost frozen neighborhood. Analysis of the mean-square displacements at longer times reveals Rouse-like dynamics with an asymptotic power law behavior $\left\langle \Delta r^2(t) \right\rangle \sim t^{0.54}$, both for the main chain and the phenyl side groups. From the long-time asymptotics the corresponding relaxation times τ_{tr} were defined. The temperature dependence of these times is described by a power law with the exponent $\gamma = 2.90$ and critical temperature $T_c =$ 380 K at $T>T_g$. At $T<T_g$ the temperature dependence of the characteristic "cage release" time is fitted by a simple activation law with the activation energy of about 30 kJ/mol for the main chain bonds and 39 kJ/mol for the phenyl groups.

The rotational mobility is investigated with the help of the time autocorrelation functions for the Legendre polynomials of the first and second order for the main-chain bonds and phenyl side groups. As in the case of translational relaxation, similar non-Arrhenius T-dependence of the relaxation times for the α-relaxation at $T>T_g$ is well reproduced. The temperature dependence of the relaxation times of the α-relaxation process follows the same power law behavior as the translational relaxation times. At $T<T_g$ the temperature dependence of the orientational relaxation times is close to the simple activation process, with the value of activation energy $E_a \sim 31$ kJ/mol, both for the main-chain bonds and side groups. Distribution function of P_2 relaxation times shows that the activated process announcing itself already at $T>T_g$.

[1] F. Beaume, B. Brulé, J.-L. Halary, F. Lauprêtre, L. Monnerie, *Polymer* **2000**, *41*, 5451.

[2] M. Baccaredda, E. Butta, V. Frosini, *Polym. Letters* **1965**, *3*, 189.

[3] O. Yano, Y. Wada, *J. Polym. Sci. A* **1971,** *9*, 669.

[4] W. Zając, B. Gabryś, D.G. Peiffer, M.A. Adams, *Physica B* **1992**, *182*, 365.

[5] T. Kanaya, T. Kawaguchi, K. Kaji, *J. Chem. Phys*. **1996,** *104*, 3841.

[6] K. Fukao, Y. Miyamoto, H. Miyaji, *J.Phys. Condens. Matter* **1991,** *3*, 5451.

[7] K. Fukao, Y. Mayamoto, *Polymer* **1993,** *34*, 238.

[8] K. Fukao, Y. Miyamoto, *J. Non-Cryst. Solids* **1994,** *172-174*, 365.

[9] A.A. Mansour, R. Junge, B. Stoll, W. Pechhold, *Colloid Polym. Sci.* **1992,** *270*, 325.

[10] A.A. Mansour, E. Happ, T. Wolf, B. Stoll, *Colloid Polym. Sci.* **1994,** *272*, 894.

[11] C. León, K.L. Ngai, C.M. Roland, *J. Chem. Phys.* **1999**, *110*, 11585.

[12] M. Wübbenhorst, A.L. de Rooij, J. van Turnhout, J. Tacx, V. Mathot, *Colloid Polym. Sci.* **2001**, *279*, 525.

[13] M.V. Vol'kenstein, A.I. Kol'tsov, A.S. Khachaturov, *Vysokomol. Soedin.* (Polymer Sci. USSR) **1965,** *7*, 296.

[14] T.M. Connor, *J. Polym. Sci. A* **1970**, *8*, 191.

[15] H.W. Spiess *Colloid Polym. Sci.* **1983**, *261*, 193.

[16] S.C. Kuebler, A. Heuer, H.W. Spiess, *Phys. Rev. E* **1997,** *56*, 741.

[17] W. Götze, in: „*Liquids, Freezing and Glass Transition*", J.P. Hansen, D.Levesque, J. Zinn-Justin, Eds., Elsevier B.V., 1991, p.287.

[18] J.D. Ferry, „*Viscoelastic Properties of Polymers*", 2nd ed., J. Wiley & Sons, New York 1970.

[19] M. Mondello et al., *Macromolecules* **1994,** *27*, 3566. H. Furuya et al., *Macromolecules* **1994**, *27*, 5674. R.J. Roe et al., *Macromolecules* **1995**, *28*, 2807.

[20] R.J. Roe *J. Non-Cryst. Solids* **1998**, *235-237*, 308.

[21] A.V. Lyulin, M.A.J. Michels, *Macromolecules* **2002**, *35*, 1463.

[22] A.V. Lyulin, M.A.J. Michels, *Comput. Phys. Commun.*, accepted.

[23] A. van Zon, A.; S.W. de Leeuw, *Phys. Rev. E* **1999**, *60*, 6942.

[24] C. Bennemann, J. Baschnagel, W. Paul, K. Binder, *Comp. Theor. Polym. Sci.* **1999**, *9*, 217.

[25] C. Bennemann, J. Baschnagel, W. Paul, *Eur. Phys. J. B* **1999**, *10*, 323.

[26] M. Aichele, J. Baschnagel, *Eur. Phys. J. E* **2001**, *5*, 229.

[27] M. Aichele, J. Baschnagel, *Eur. Phys. J. E* **2001**, *5*, 245.

[28] G. Ciccotti, M. Ferrario, J.P. Ryckaert, *Mol. Phys.*, **1982**, *47*, 1253.

[29] M.P. Allen, D.J. Tildesley, „*Computer Simulation of Liquids*", Clarendon Press, Oxford, 1987.

[30] S. Provencher; V. Dovi, *J. Biochem. Biophys. Methods* **1979**, 1, 313.

[31] S. Provencher, *Comput. Phys. Commun.* **1982**, 27, 213.